Fabrication of Co(OH)F Catalyst for Efficient Peroxymonosulfate Activation in Sulfamethazine Degradation

Chengli Zhang [a], Yonglei Xing [a, *], Xiaoyong Jin [a, *], Yage Peng [a], Gang Ni [b, *]

[a] State Key Laboratory of High-efficiency Utilization of Coal and Green Chemical Engineering, National Demonstration Center for Experimental Chemistry Education, School of Chemistry and Chemical Engineering, Ningxia University, Yinchuan, 750021, PR China.

[b] Ningxia Key Laboratory of Green Catalytic Materials and Technology, College of Chemistry and Chemical Engineering, Ningxia Normal University, Guyuan 756000, PR China

---

* Corresponding author:
Tel.: +86-0951-2062851 (O), Fax: +86-0951-2062851, Email address: ylxing@nxu.edu.cn; jinxy588@163.com; nigang@nxu.edu.cn.

1. Characterization

The crystal structure of the sample was characterized by X-ray diffraction (XRD) using a Bruker D8 Advance diffractometer with Cu Kα radiation ($\lambda = 1.5406$ Å) operated at 40 kV and 40 mA. Data were collected from the solid powder sample in the 2θ range of 10°–80° with a step size of 0.01°. Phase identification and analysis were performed using the MDI Jade software package. Sample morphology was examined using a ZEISS Sigma 300 field-emission scanning electron microscope (SEM). Prior to imaging, the samples were sputter-coated with a thin layer of gold and observed under a 5 kV accelerating voltage in secondary electron (SE2) mode. Transmission electron microscopy (TEM) analysis was performed on a JEOL JEM-F200 field-emission microscope at an accelerating voltage of 200 kV. The sample was prepared by ultrasonic dispersion in ethanol, followed by depositing the suspension onto an ultra-thin carbon-coated copper grid and drying. Bright-field images, high-resolution transmission electron microscopy (HRTEM) images, and energy-dispersive X-ray spectroscopy (EDS) mapping were acquired for qualitative elemental analysis and elemental distribution assessment. The elemental composition and chemical states of the sample surface were analyzed using X-ray photoelectron spectroscopy (XPS) with a Thermo Fisher Scientific Nexsa spectrometer. High-resolution spectra were acquired with a pass energy of 50.0 eV and an energy step size of 0.100 eV. The binding energy scale was calibrated by referencing the adventitious carbon C 1s peak to 284.8 eV. Data analysis was performed using Thermo Avantage software, employing a Shirley-type background subtraction and peak deconvolution with a Gaussian-Lorentzian (30% Lorentzian) function. The surface functional groups of the sample were examined by Fourier-transform infrared spectroscopy (FT-IR) using a Bruker INVENIO spectrometer equipped with a diamond attenuated total reflectance (ATR) accessory. Measurements were performed directly on the solid sample without further preparation. Spectra were collected and processed using the Bruker OPUS software.

Textural parameters, including specific surface area, pore-size distribution, and nitrogen adsorption–desorption isotherms, were obtained using a surface area and porosity analyzer (Micromeritics ASAP 2460) based on the Brunauer–Emmett–Teller (BET) method. Surface charge characteristics were measured using a Zeta potential analyzer (POWEREACH JS94H2). Sulfamethazine (SMZ) concentrations were quantified by high-performance liquid chromatography (HPLC, HITACHI, Japan), and degradation intermediates were determined by ultra-high-performance liquid chromatography coupled with an Orbitrap high-resolution mass spectrometer (LC–MS, Thermo Fisher LTQ Orbitrap XL, USA). Reactive species capture tests were performed using electron paramagnetic resonance spectroscopy (EPR, JES-X310, JEOL, Japan). Thermal stability was assessed via thermogravimetric analysis (TGA) on a Discovery TGA 55 instrument (TA Instruments, USA). Chemical oxygen demand (COD) was measured with a multiparameter water quality analyzer (Lianhua Technology, China).

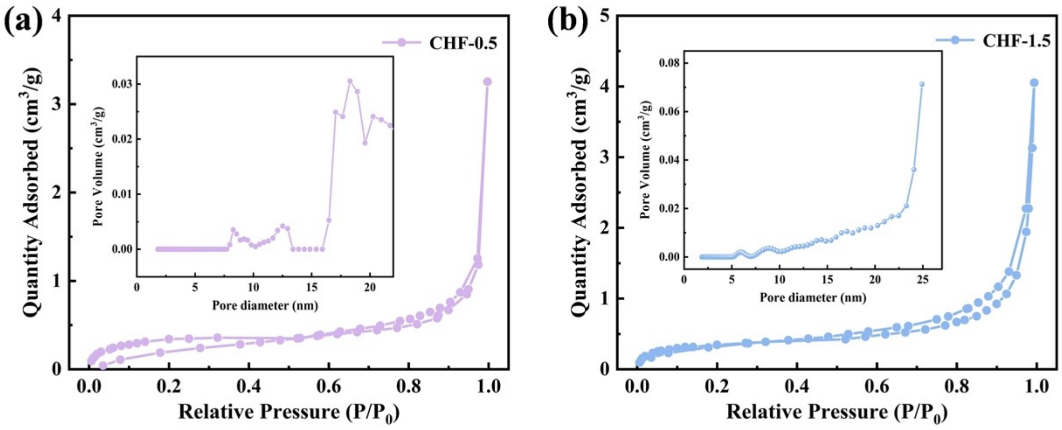

Fig. S1. Nitrogen adsorption–desorption isotherms and corresponding pore size distributions (insets) of (a) CHF-0.5 and (b) CHF-1.5.

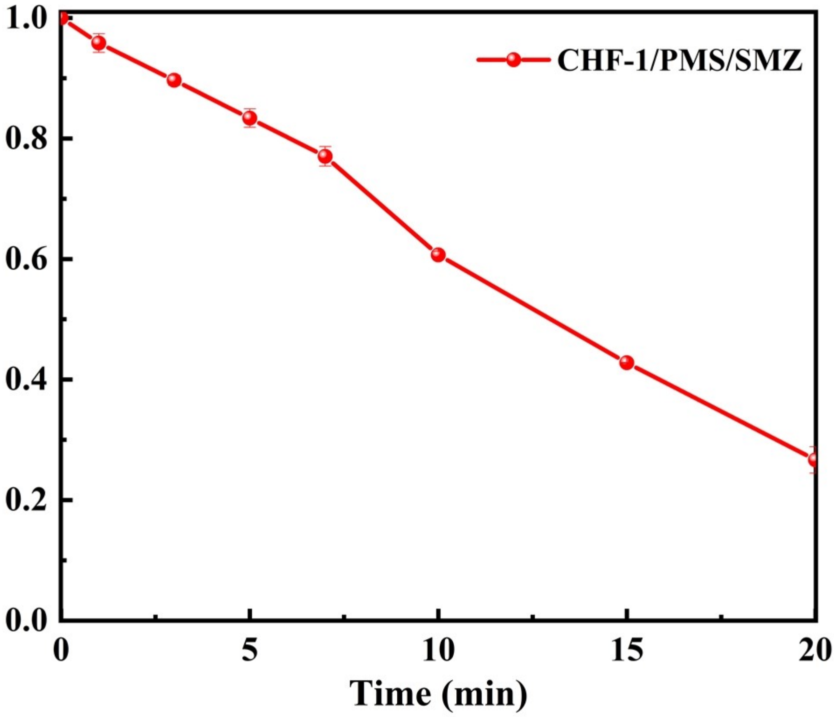

Fig. S2. Residual PMS concentrations in the CHF-1/PMS/SMZ reaction system.

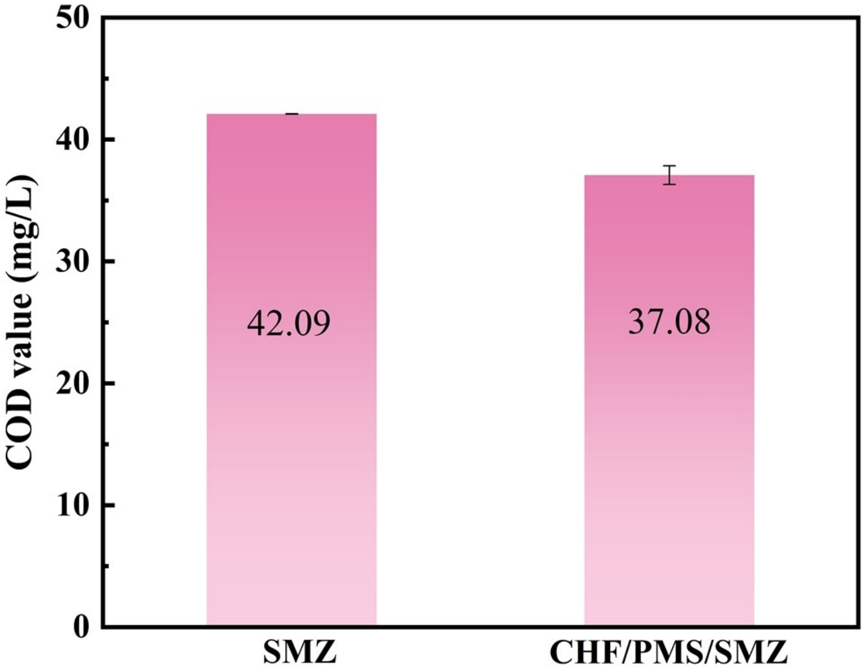

Fig. S3. COD values of different reaction systems.

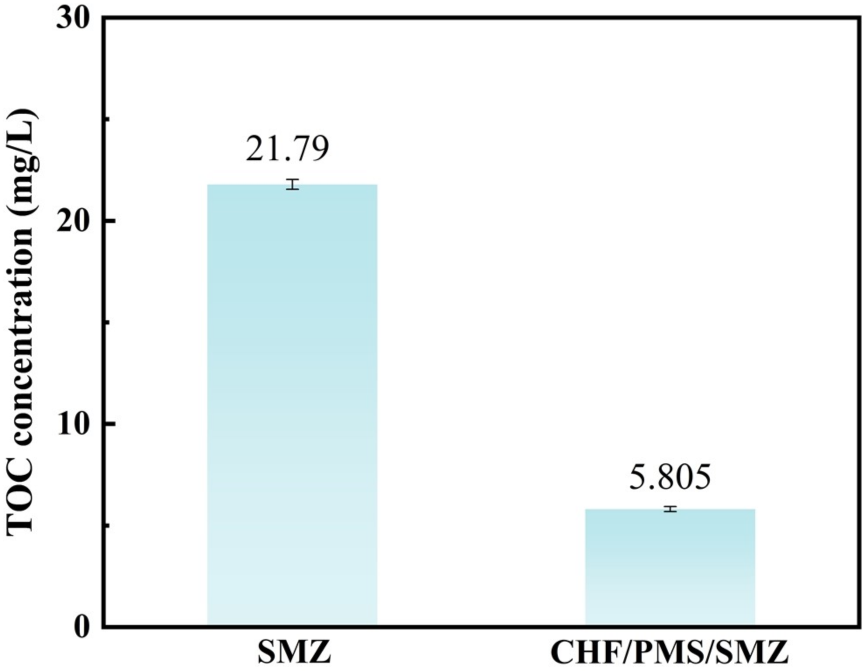

Fig. S4. TOC concentrations of different reaction systems.

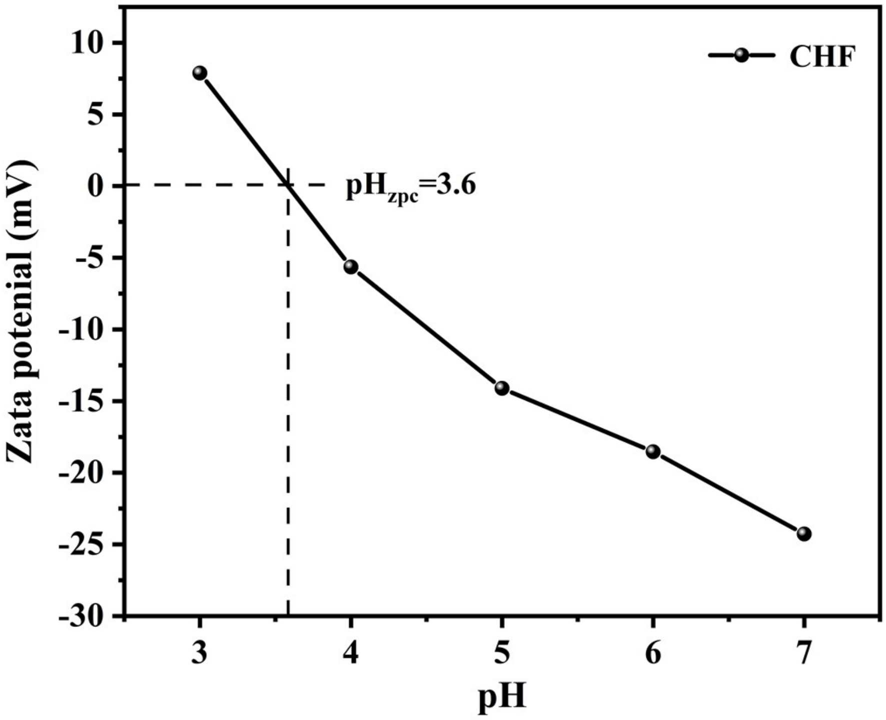

Fig. S5. Zeta potential of the catalyst at various pH values.

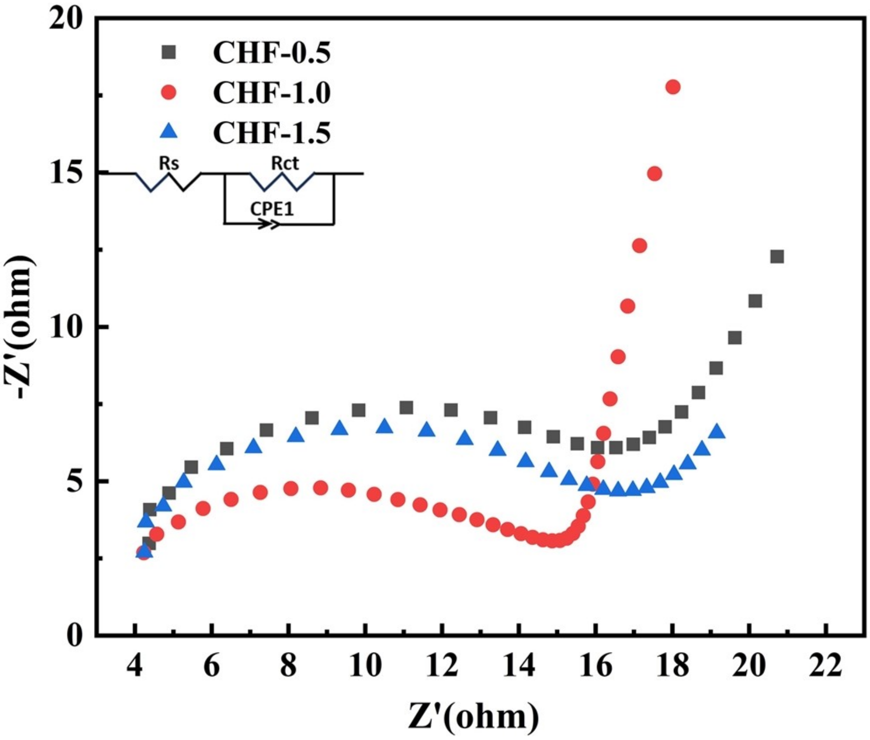

Fig. S6. EIS spectra of different catalysts.

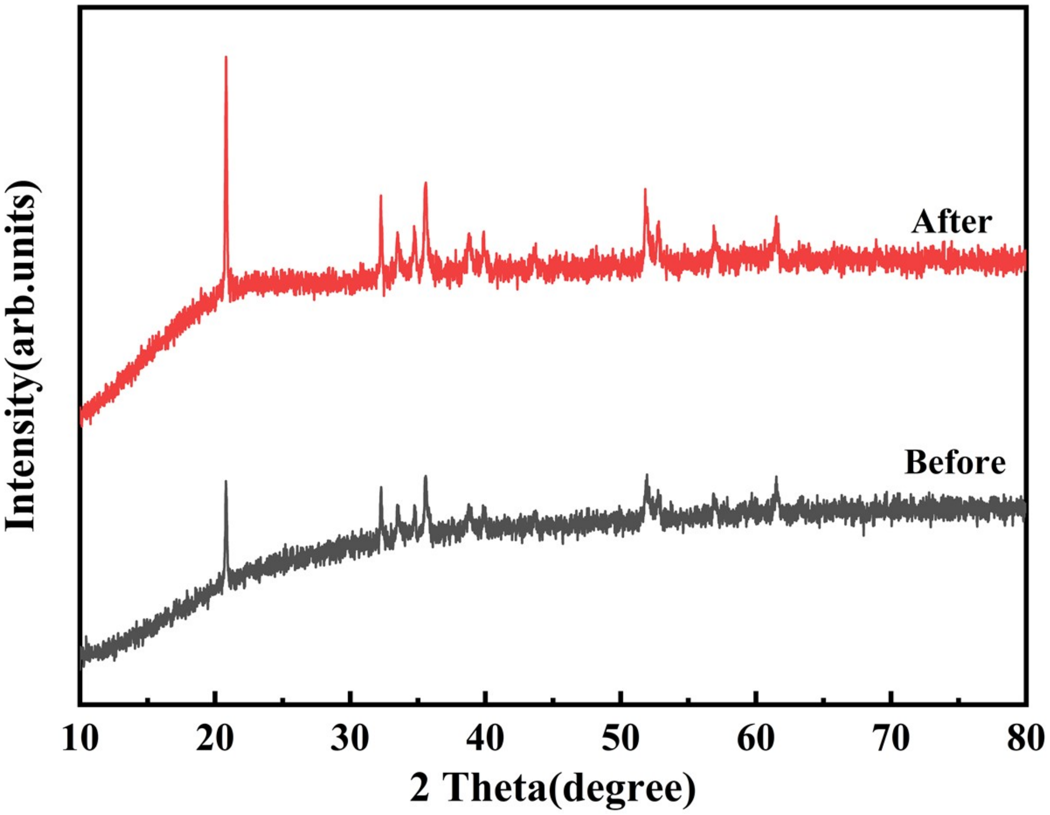

Fig. S7. XRD patterns of CoOHF-1 before and after the reaction.

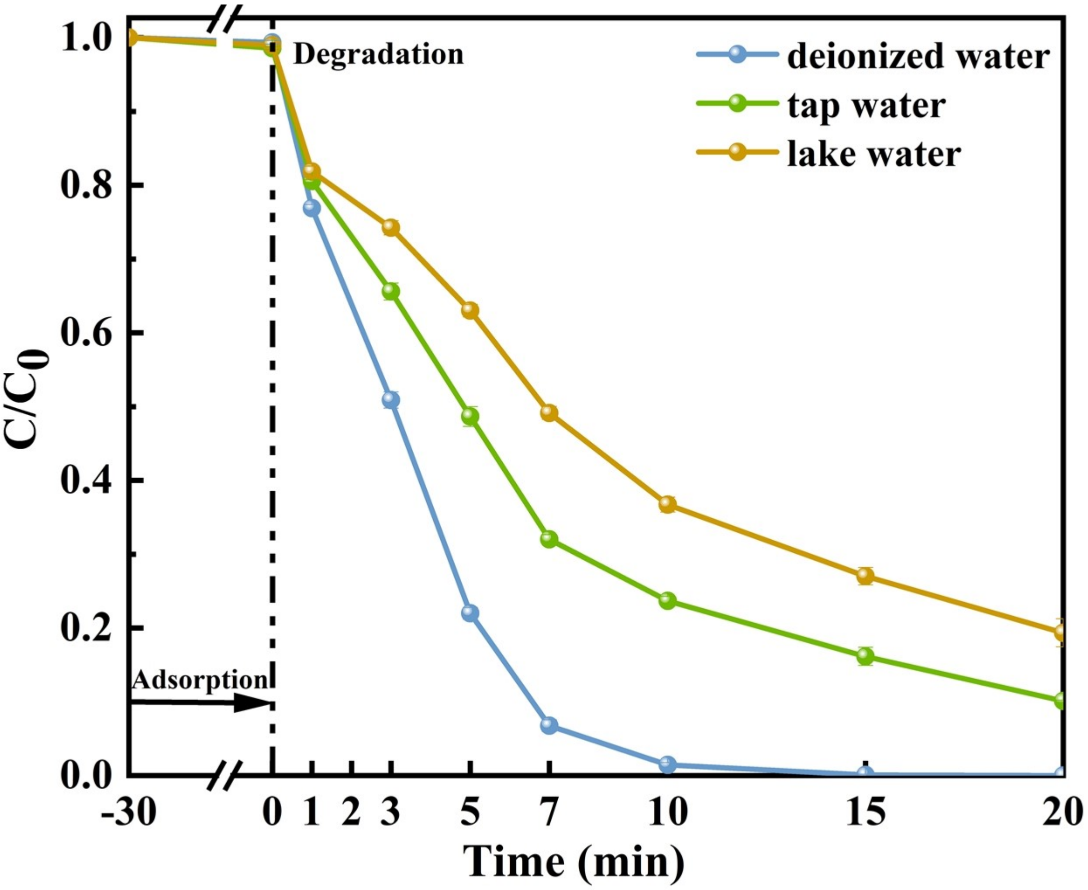

Fig. S8. Effect of different water matrices on SMZ degradation efficiency.

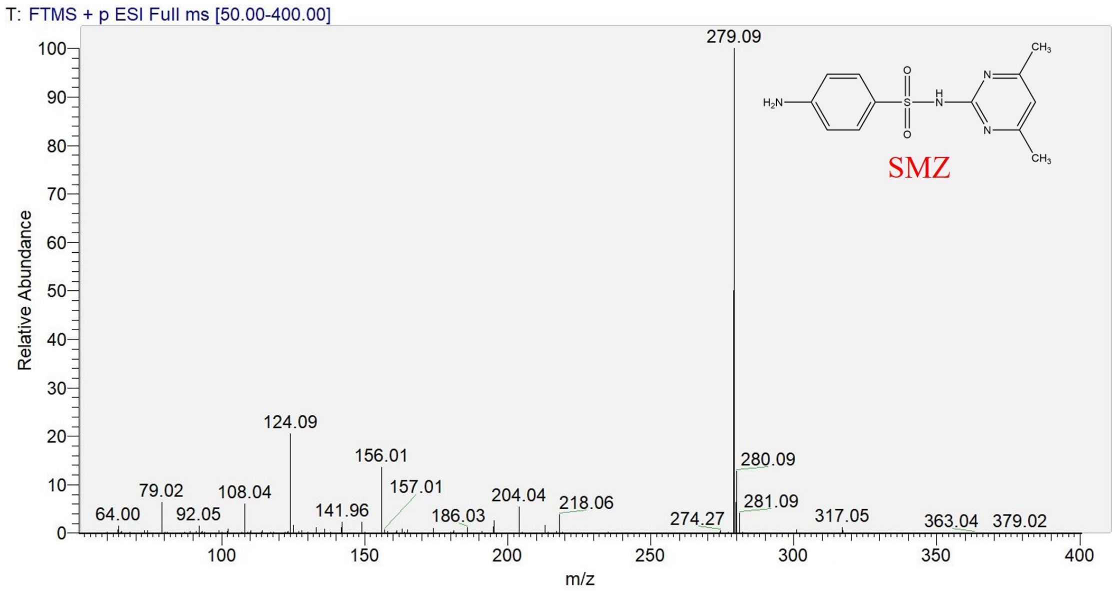

Fig. S9. Mass spectrum of intermediates detected during SMZ degradation.

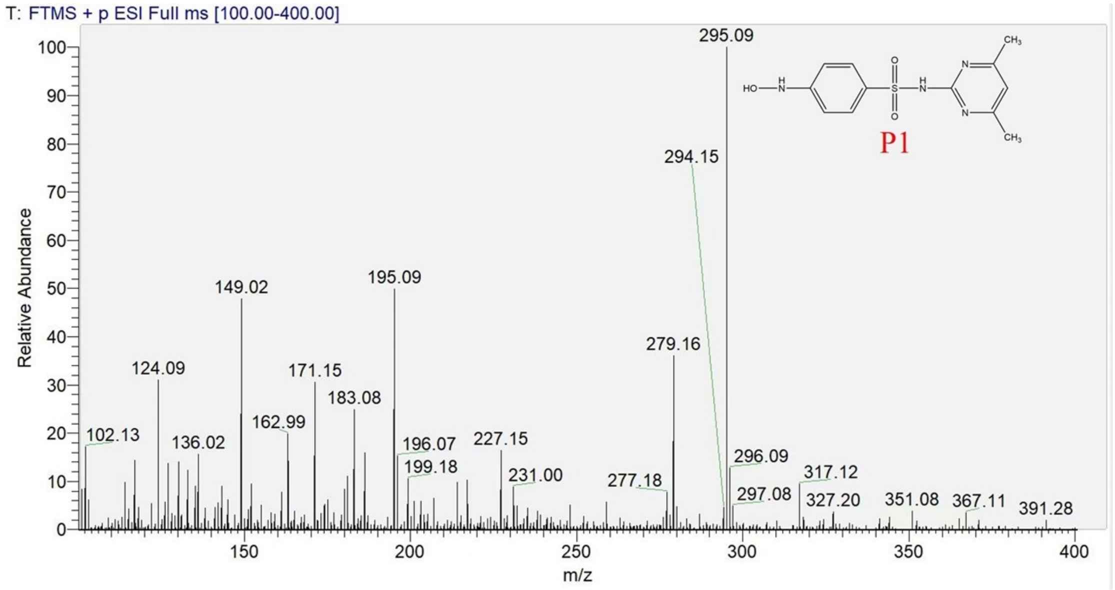

Fig. S10. Mass spectrum of intermediate P1 detected during SMZ degradation.

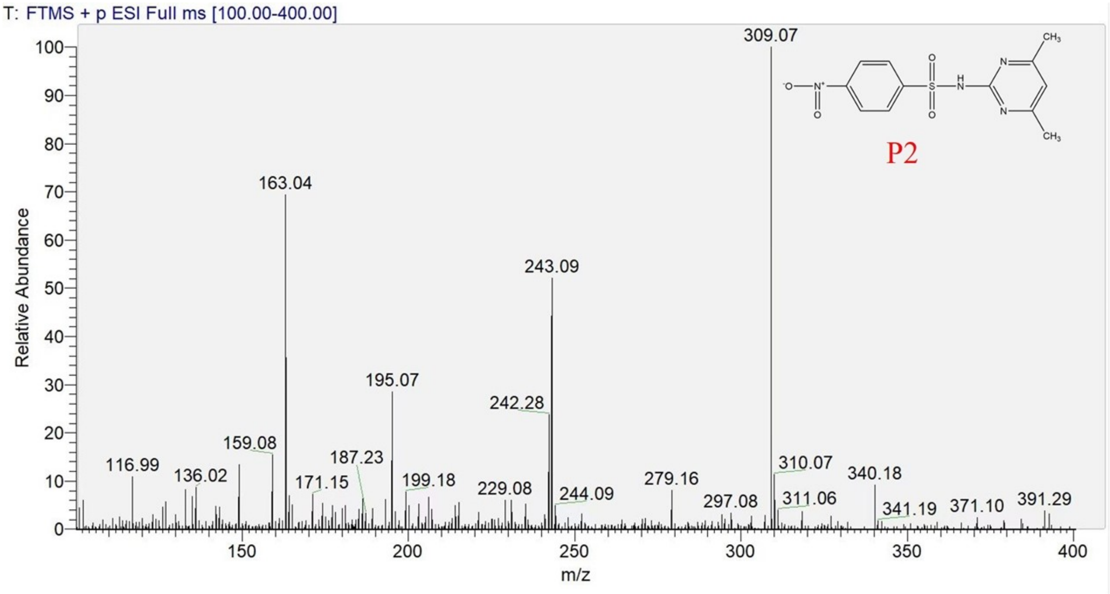

Fig. S11. Mass spectrum of intermediate P2 detected during SMZ degradation.

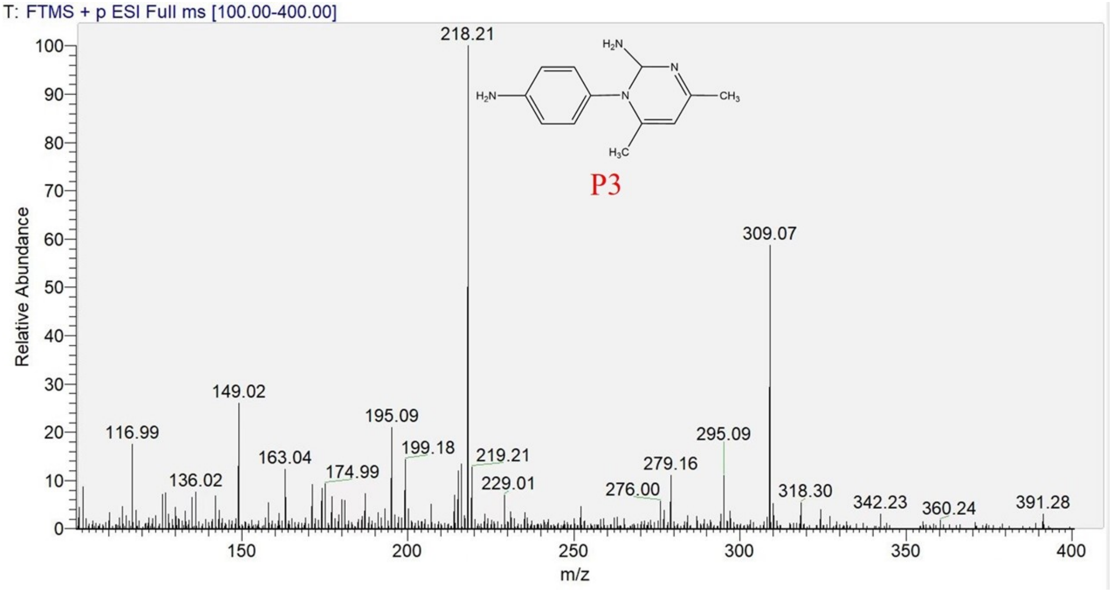

Fig. S12. Mass spectrum of intermediate P3 detected during SMZ degradation.

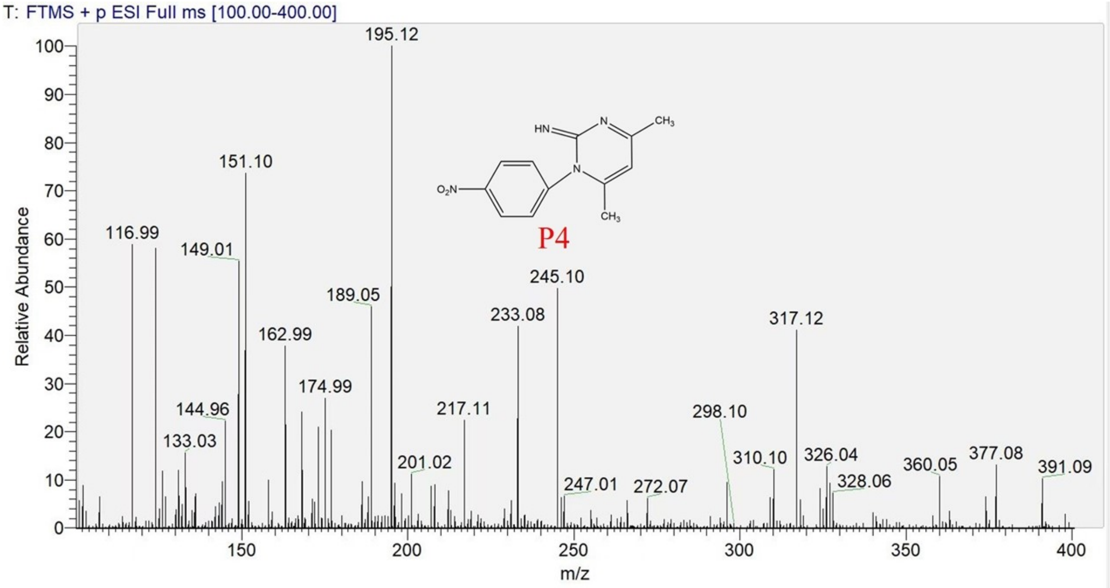

Fig. S13. Mass spectrum of intermediate P4 detected during SMZ degradation.

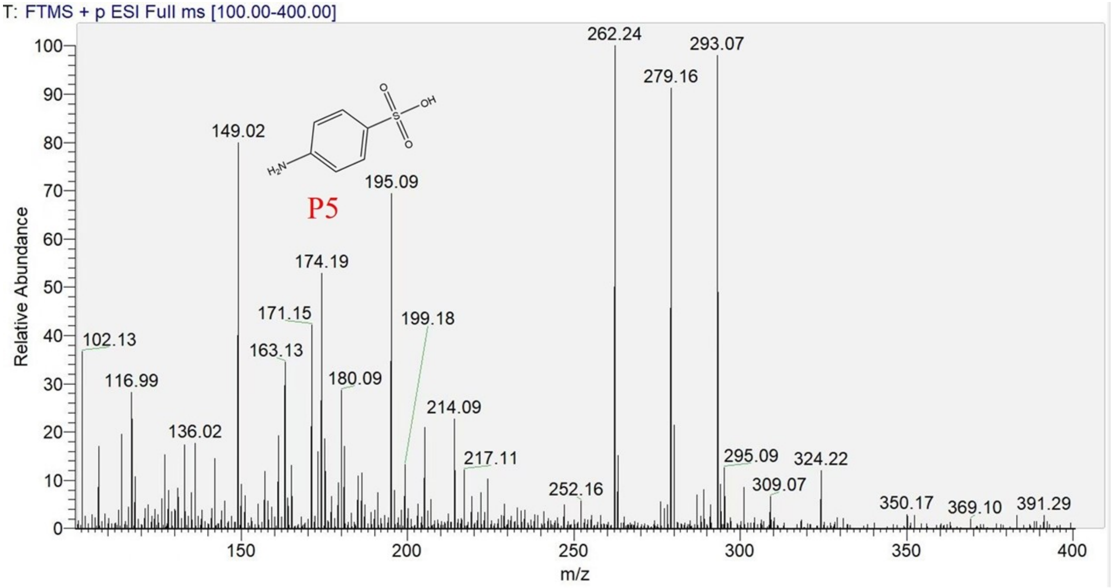

Fig. S14. Mass spectrum of intermediate P5 detected during SMZ degradation.

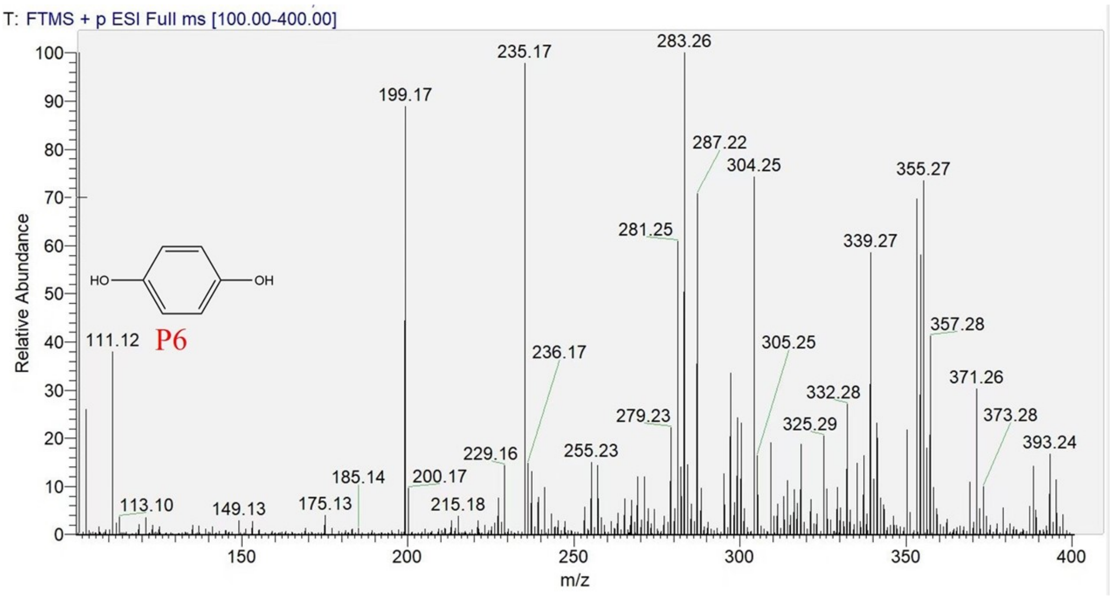

Fig. S15. Mass spectrum of intermediate P6 detected during SMZ degradation.

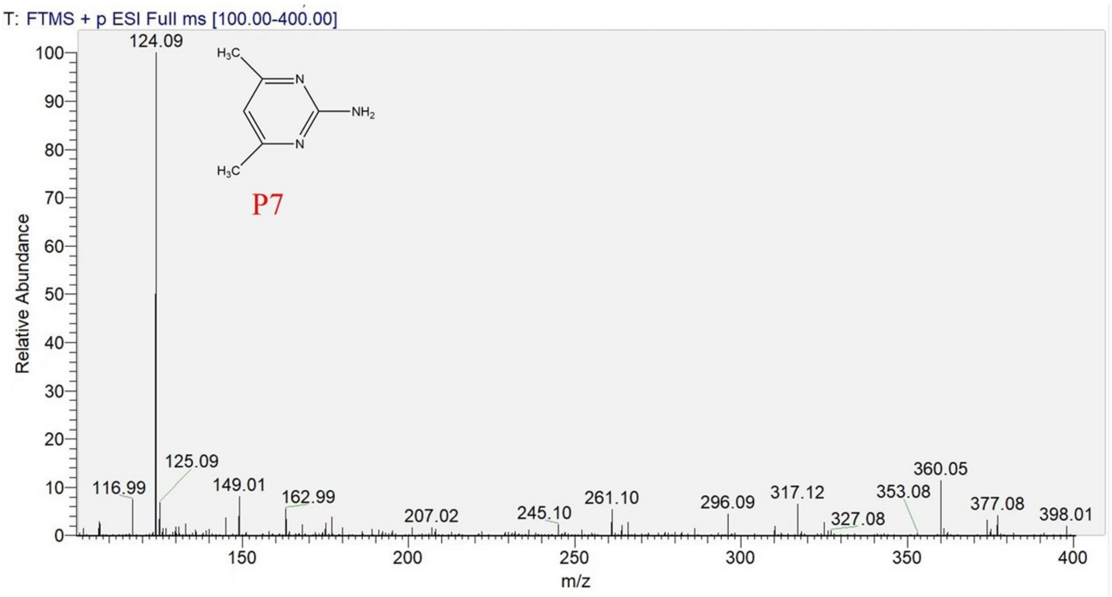

Fig. S16. Mass spectrum of intermediate P7 detected during SMZ degradation.

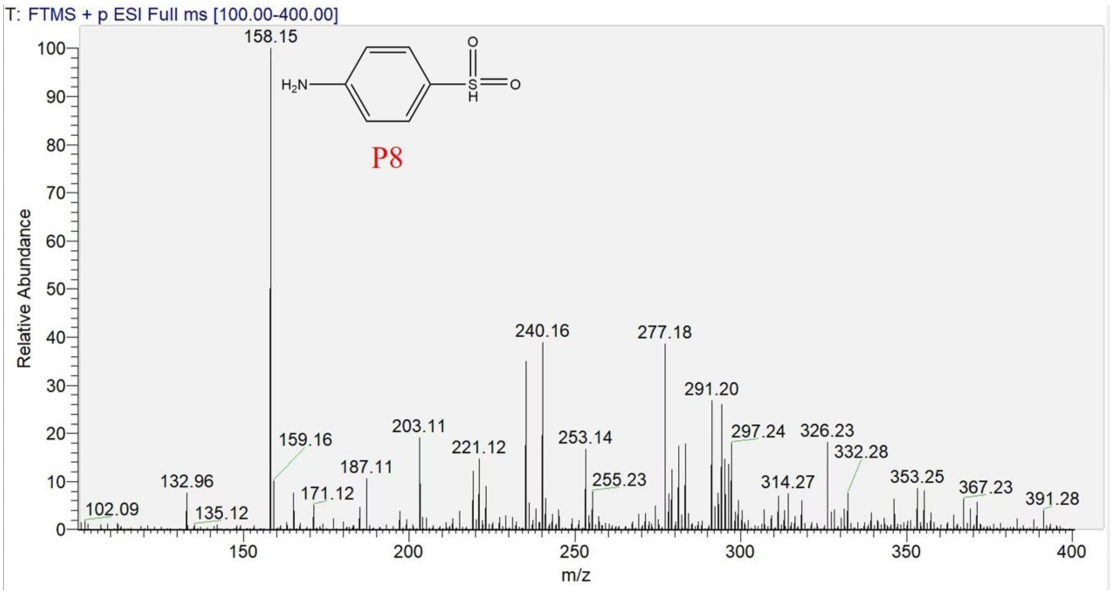

Fig. S17. Mass spectrum of intermediate P8 detected during SMZ degradation.

Table. S1. List of chemical reagents used in this study.

Chemical reagents	**Specifications**	**Manufacture**
Cobalt(II) nitrate hexahydrate $Co(NO_3)_2{\cdot}6H_2O$	AR	Aladdin Chemical Reagent Co., Ltd
Ammonium fluoride (NH_4F)	98%	Aladdin Chemical Reagent Co., Ltd
Hexamethylenetetramine (HMTA)	AR	Sinopharm Chemical Reagent Co., Ltd.
Sodium thiosulfate ($Na_2S_2O_2$)	AR	Aladdin Chemical Reagent Co., Ltd
Sulfamethazine (SMZ)	≥ 99%	Aladdin Chemical Reagent Co., Ltd
Carbamazepine (CBZ)	≥ 98%	Aladdin Chemical Reagent Co., Ltd
Bisphenol F (BPF)	≥ 99%	Macklin Biochemical Co., Ltd.
Tetracycline (TC)	≥ 99%	Aladdin Chemical Reagent Co., Ltd
Ciprofloxacin (CIP)	≥ 99%	Macklin Biochemical Co., Ltd.
Isopropanol (IPA)	AR	Sinopharm Chemical Reagent Co., Ltd.
Furfuryl alcohol (FA)	≥ 97%	Aladdin Chemical Reagent Co., Ltd
Dimethyl sulfoxide (DMSO)	≥ 99%	Aladdin Chemical Reagent Co., Ltd
p-Benzoquinone (p-BQ)	≥ 99%	Macklin Biochemical Co., Ltd.
Humic acid (HA)	≥ 90%	Aladdin Chemical Reagent Co., Ltd
5,5-Dimethyl-1-pyrroline-N-oxide (DMPO)	AR	Sigma-Aldrich
,2,6,6-Tetramethylpiperidine (TEMP)	AR	Sigma-Aldrich
Peroxymonosulfate (PMS)	4.5% active content	Sinopharm Chemical Reagent Co., Ltd.

Table S2. Specific surface area, total pore volume, and average pore diameter of the samples.

Sample	S_{BET} (m^2/g)	Pore volume (cm^3/g)	Average pore size (nm)
CHF-0.5	1.2861	0.004458	8.4469
CHF-1.0	1.5997	0.006754	10.6290
CHF-1.5	1.2628	0.006083	12.4994

Table S3. Reported SMZ degradation performances in activated persulfate systems.

Catalyst (Dosage)	PMS (Concentration)	Pollutant (mg/L)	Removal efficiency	K_{obs} (min^{-1})	K-value ($min^{-1}\cdot g^{-1}$)	Mechanism	Ref.
$CuCo_2O_4$ spinel (0.01 g/L)	0.02 (g/L)	5	87.2% (20 min)	0.107	10.7	Co^{2+}, Cu^{2+}	[1]
rGO-CNCF (0.2 g/L)	0.1 (g/L)	10	99.9% (30 min)	0.292	1.46	visible light, $^1O_2$	[2]
H_2-reduced hematite (0.2 g/L)	0.2 (g/L)	10	99.3% (20 min)	0.135	0.675	$SO_4^{\cdot-}$, ·OH	[3]
$BC\text{-}FM_{0.25}$ (0.5 g/L)	0.5 (g/L)	50	98% (30 min)	0.170	0.34	electron transfer	[4]
Mn_3Fe_1−NC (0.05 g/L)	1.5 (mM)	5	91.8% (90 min)	0.0263	0.526	electron transfer	[5]
Co@MoS_2 (0.5 g/L)	10 (mM)	10	100% (10 min)	0.531	1.062	Co^{2+}, $^1O_2$	[6]
Co@NC (0.05 g/L)	0. 25 (mM)	20	100% (20 min)	0.334	6.68	Co(IV), $^1O_2$	[7]
Co@MGA (0.3 g/L)	1 (mM)	20	90% (10 min)	0.05815	0.194	electron transfer, $^1O_2$	[8]
CoOHF (0.2 g/L)	0.6 (mM)	20	100% (10 min)	0.999	4.995	$SO_4^{\cdot-}$, $^1O_2$	**This work**

Table S4. Transformation products identified during SMZ degradation by LC–MS analysis.

Compound	Detected mass (m/z)	Chemical Formula	Molecular Structure
SMZ	279.09	$C_{12}H_{14}N_4O_2S$	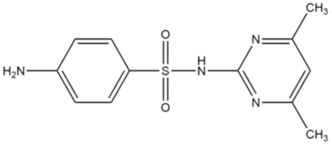
P1	295.09	$C_{12}H_{14}N_4O_3S$	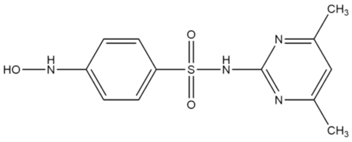
P2	309.07	$C_{12}H_{12}N_4O_4S$	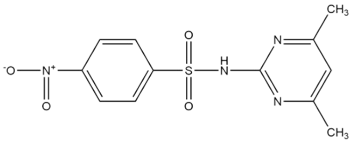
P3	218.21	$C_{12}H_{16}N_4$	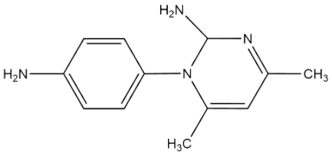
P4	245.10	$C_{12}H_{12}N_4O_2$	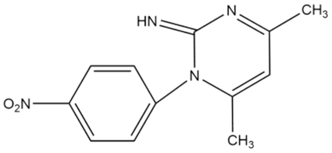
P5	174.19	$C_6H_7NO_3S$	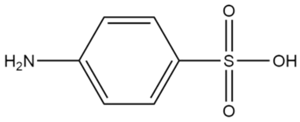
P6	111.12	$C_6H_6O_2$	
P7	124.09	$C_6H_9N_3$	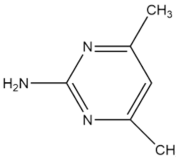
P8	158.15	$C_6H_7NO_2S$	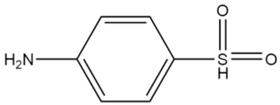

Table S5. Predicted ecotoxicity of SMZ and its degradation products evaluated by the T.E.S.T. software.

Compound	**Acute toxicity（mg/L）**		**Bioconcentration factor**	**Developmental toxicity**	
	Daphnia magna LC_{50} (48 h)	Fathead minnow LC_{50} (96 h)	Predicted value	Predicted value	Predicted result
SMZ	29.55	4.74	2.35	0.90	Developmental toxicant
P1	30.37	3.31	3.01	0.89	Developmental toxicant
P2	21.67	0.82	5.53	0.92	Developmental toxicant
P3	0.58	19.64	12.74	0.72	Developmental toxicant
P4	1.95	1.60	34.30	1.01	Developmental toxicant
P5	14.35	143.01	2.50	0.45	Developmental NON-toxicant
P6	13.51	43.29	13.43	0.52	Developmental toxicant
P7	8.21	404.20	3.03	0.68	Developmental toxicant
P8	8.44	81.49	2.95	0.36	Developmental NON-toxicant

white boxes, not harmful: LC50(48h) >10 mg/L , LC50(96h) > 100 mg/L; yellow boxes, harmful: 10 mg/L ≥ LC50(48h) > 1 mg/L, 100 mg/L ≥ LC50(96h) > 10 mg/L; orange boxes, toxic: 1 mg/L ≥ LC50(48h) ≥0.1 mg/L, 10 mg/L ≥ LC50(96h) ≥ 1 mg/L; red boxes, highly toxic: LC50(48h) < 0.1 mg/L, LC50(96h) < 1 mg/L.